BEHAVIOR OF STEEL-CONCRETE COMPOSITE BEAMS STRENGTHENED WITH UNSTRESSED AND PRESTRESSED HIGH-MODULUS CFRP STRIPS

David Schnerch, Mina Dawood, Emmett A. Sumner, and Sami Rizkalla
Department of Civil, Construction, and Environmental Engineering, North Carolina State University, Raleigh, NC, USA

ABSTRACT

Substantial demand exists for strengthening steel bridges and structures. The potential for using high modulus CFRP strips for strengthening has been shown through a multi-phase research program. A feasibility study was first conducted using large-scale members that were strengthened with unstressed and prestressed CFRP strips using intermediate and high modulus fibers. These fibers had a tensile modulus up to three times that of steel. The behavior of strengthened steel-concrete composite beams has also been investigated under conditions of overloading and to determine the significance of shear-lag. Further work is in progress in the area of fatigue.

Keywords: *flexural strengthening, overloading, prestressed, shear-lag, steel bridges*

1. INTRODUCTION

1.1 Research Objective

Severe deterioration of steel bridge girders in service, in conjunction with demands for increases in allowable truck weights and limited funding for new bridge structures, has created the demand for a reliable and durable system for strengthening these structures. A feasibility study was initially conducted to determine the potential to strengthen and provide stiffness increases at service load levels for steel-concrete composite beams that are typical of bridge structures. This work involved the use of new, high modulus, CFRP materials. Continuing work is now focused on addressing the problems of shear-lag, overloading and fatigue for steel members strengthened with these high modulus CFRP materials.

1.1.1 Previous Work

Considerable previous work has been focused on the use of standard modulus CFRP materials for strengthening of steel structures. Several studies have shown the

possibility of strengthening steel girders with CFRP materials (Edberg *et al*., 1996), repairing corroded girders removed from service (Gillespie *et al*., 1996) or repair of girders that simulated corrosion by reduction of the cross-section (Liu *et al*., 2001 and Tavakkolizadeh and Saadatmanesh, 2001A). While these studies have shown significant increases in the ultimate strength or restoration to the original strength for corroded sections, no significant increase in stiffness in the service range has been observed. This is due to the similar stiffness between the CFRP strips used in these studies and the steel, which requires that a great deal of strengthening be applied. However, the efficiency of any bonded system decreases as strip thickness increases or multiple plys are used. Use of higher modulus CFRP material has the potential to provide stiffness increases in the service range, using strips of a reasonable thickness.

1.1.2 Fatigue

Research on the fatigue behavior of steel girders strengthened or repaired with CFRP laminates has been limited. Two girders taken from a decommissioned bridge were strengthened with CFRP laminates and tested in fatigue to 10 million cycles at a stress range of 34 MPa to simulate a condition more severe than a typical field application. No evidence of debonding was observed and the overall member stiffness was unaffected by the fatigue loading (Miller *et al*., 2001). In another study, 21 small-scale beams were artificially notched to simulate fatigue cracking. Six were then repaired with CFRP laminates, and all of the beams were tested in medium cycle fatigue at stress ranges between 69 MPa (0.28 f_y) and 379 MPa (1.53 f_y). The testing demonstrated that fatigue life could be increased between 2.6 and 3.4 times by adhesive bonding of CFRP laminates effectively upgrading the specimens from AASHTO category D to AASHTO category C. Application of the CFRP patch also reduced stable crack growth rates by 65% on average (Tavakkolizadeh and Saadatmanesh, 2003B).

1.1.3 Durability and Galvanic Corrosion

Galvanic corrosion has the potential to not only accelerate corrosion of the steel, but also degrade the CFRP material itself (Miriyala *et al.*, 1992). There are three necessary conditions for the formation of galvanic corrosion: an electrolytic solution must bridge the two materials, there must be direct electrical connection between the materials and there must be a sustained cathodic reaction on the carbon (Francis, 2000). By preventing any one of these conditions from occurring, galvanic corrosion cannot occur. Preventing more than one of these conditions from occurring results in a "safety factor," should one of the prevention mechanisms fail.

Most of the research has been focused on the prevention of direct contact between the steel and the carbon fiber material. Barrier layers of adhesive, or the incorporation of a GFRP layer have been shown to be effective in preventing galvanic corrosion (Brown, 1974 and Tavakkolizadeh and Saadatmanesh, 2001B). However, Choqueuse *et al.* (1997) has shown greater moisture uptake for GFRP materials than for the neat resin alone. Gellert and Turley (1999) also observed degradation of the interface between glass fibers and epoxy resin. In this case, alkali metal oxides were leached from the E-glass fibers, resulting in a concentrated solution being formed at the interface surrounding the fibers. The concentration gradient between the interface,

where the solution is most concentrated, and the surrounding resin resulted in further diffusion of water towards the fiber-matrix interface.

Rather than focusing on the prevention of galvanic corrosion by incorporation of GFRP barrier layers, it may be as important to prevent moisture, in the form of electrolytic solutions, from coming into contact with the bonded material. This may be accomplished with the addition of different types of coatings or sealers applied to the surface. Apart from the problems of galvanic corrosion, moisture penetration into the bonded repair can also affect the interface between the steel and the adhesive where the chemical bonds are primarily secondary bonds (Mays and Hutchinson, 1992) and can cause plastification of the matrix (McBagonluri *et al*., 2000).

1.2 High Modulus Carbon Fiber Material

Two types of unidirectional, pultruded CFRP strips were used in the experimental program. Diversified Composites custom pultruded the CFRP strips, designated DC-I, using an intermediate modulus DIALEAD K63312 fiber produced by Mitsubishi Chemical America, Inc. Epsilon Composite manufactured the other type of strip, using the higher modulus DIALEAD K63712 fiber, designated THM-450, which was a standard product. Material properties for the strips produced by Diversified Composites were determined by the producer. An external laboratory, determined the properties for the strips produced by Epsilon Composites. The values given for the THM-450 strips are the average of tests results for the same type of strip pultruded to two different thicknesses. These values are listed in Table 1.

Table 1 Properties for the two types of CFRP strips used in the experimental program

Property	DC-I	THM-450
Strip thickness (mm)	3.2	2.9 or 4.0
Fiber volume fraction (%)	55.4%	70%
Tensile strength (MPa)	1224	1534
Tensile modulus (GPa)	229	457
Ultimate elongation (percent)	0.508	0.332

2. EXPERIMENTAL PROGRAM

2.1 Phase 1: Large-Scale Steel-Concrete Composite Beams

2.1.1 Test Specimens

The experimental program included three large-scale beam specimens that were fabricated from grade A992 steel W310 x 45 sections, 6550 mm in length. These beams had an average yield strength of 373 MPa. Shear studs that were 76 mm in length and 19 mm in diameter were welded at a spacing of 152 mm along the length of the compression flange to ensure full composite action between the concrete deck and the steel section. These studs were also staggered to minimize the possibility of deck splitting. Concrete strength, determined at the time of testing, varied between 37 and 44 MPa for all the large-scale beams. Longitudinal reinforcement of the deck consisted of grade 60 steel bars that were 12.7 mm in diameter. The spacing of the

longitudinal concrete reinforcement varied as shown in Fig. 1 and was continuous over the full length of the beam. Transverse reinforcement, using the same bars, was provided at a constant spacing of 152 mm. All the reinforcing bars were determined to have a yield strength of between 436 and 463 MPa using the 0.2% offset method.

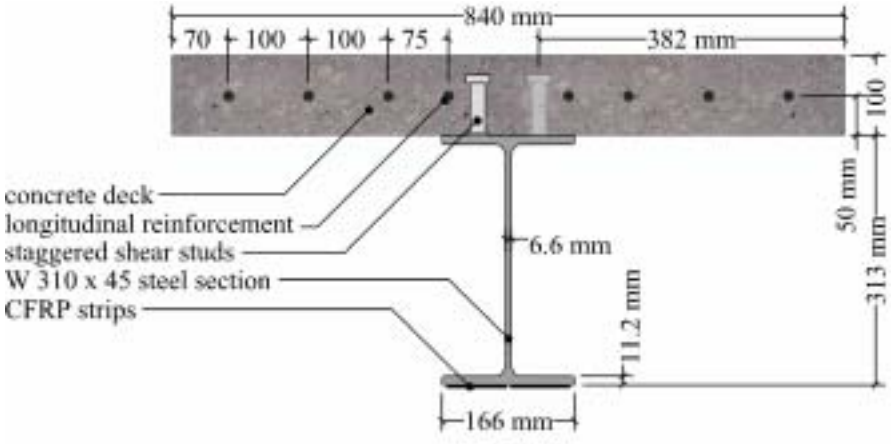

Fig. 1 Cross-section dimensions for large-scale steel-concrete composite beams

Different strengthening configurations were used for each of the three specimens. The designation of each specimen was given based on three different parameters. The first parameter indicated the modulus of the fiber used for the strengthening, whether intermediate modulus or high modulus. The second parameter gives the reinforcement ratio of the applied strengthening, defined as the cross-sectional area of longitudinal fiber, taking into account the fiber volume fraction of the strips used, divided by the cross-sectional area of the steel section. The final parameter lists whether the strengthening was adhesively bonded without stressing the CFRP strips or if it was first prestressed. The test matrix is listed in Table 2.

Table 2 Test matrix for large-scale steel-concrete composite beam specimens

Designation	CFRP type	Reinforcement ratio	Application method
IM-4.5-AB	DC-I	4.5%	adhesive bonded CFRP strips
HM-7.6-AB	THM-450	7.6%	adhesive bonded CFRP strips
HM-3.8-PS	THM-450	3.8%	prestressed CFRP strips

To prepare the beams for strengthening, each beam was sandblasted along the underside of the tension flange. Sandblasting and the longitudinal strengthening were conducted in a single day to minimize oxidation of the freshly sandblasted steel surface. Following sandblasting, dust was removed from the surface of the beam by blowing with compressed air, then brushing with acetone. Acetone was applied in excess so that it dripped from the beam, removing any dissolved particles rather than redistributing them once the acetone had evaporated.

The one beam specimen that used, the DC-I type of strip, was manufactured with no peel ply and had a smooth shiny surface. To ensure adequate adhesion of the epoxy to

the surface of the CFRP material, these strips were lightly hand sanded with 120 grit sandpaper. The surface of the strips was cleaned by wiping with methanol. The remaining beams using the THM-450 strips were manufactured with a glass-fiber peel-ply and a rough-textured surface. No surface preparation of the strip was necessary after removal of the peel-ply. For both types of strips, a 20-degree taper was machined with a special fixture and a belt-type sander. The strips were then applied to the beams, such that the adhesive bondline thickness was locally increased in the region of the taper. Hildebrand (1994) showed that the stress concentration that typically occurs near the strip edge for bonded joints can greatly reduced by providing a reverse taper at the ends. All of the specimens used Spabond 345 epoxy resin, manufactured by SP Systems. Specimens were allowed to cure for at least seven days following application of the CFRP strips before testing was completed.

For the beam using the prestressed strips, several steps were completed before applying the CFRP strips. Special steel tabs were fabricated that would be used to apply the prestressing force. The CFRP strips were bonded to the steel tabs at their ends and left to cure for seven days. Prior to sandblasting the beam, holes were drilled into the bottom flange of the beam to accept the tab used at the fixed-end and the fixture used to apply the jacking force. After the surface preparation of the beam was complete, adhesive was applied to the entire CFRP strip on the side that would be in contact with the beam and additional epoxy was applied directly to the soffit of the beam. The steel tab at the fixed end was first bolted to the steel beam. Next, the tab at the other end of the CFRP strip was inserted into the fixture to apply the prestressing force, by means of tightening threaded rods that were positioned one on each side of the beam. These threaded rods were located at the same level as the CFRP strip to avoid twisting of the tabs.

Prestressing force was monitored by the use of strain gauges that were bonded to the CFRP strips at midspan. The threaded rods were tightened evenly on both sides, until the design prestressing strain of 0.06 percent was achieved. The strips were then clamped to the surface of the steel beam using the same procedure that had been used for the non-prestressed beams.

2.1.2 Test Procedure

The large-scale steel-concrete composite beam specimens, spanning 6400 mm, were tested in four-point bending under displacement control, as shown in Fig. 2, with loads applied symmetrically about the center of the span. Neoprene pads were used at the supports and under the load points to allow for rotation. Loading was applied across the full width of the concrete slab by the use of 150 mm deep steel HSS sections that were placed between the spreader beam and the neoprene pads. Each of the beams was subjected to three loading cycles. The first cycle of loading, was to induce a strain of 0.12 percent (or about 60 percent of the yield stress) at the level of the tension flange before the beam was strengthened. After strengthening and curing of the adhesive, the next loading was to the same stress. Finally, the beam was reloaded to its ultimate strength.

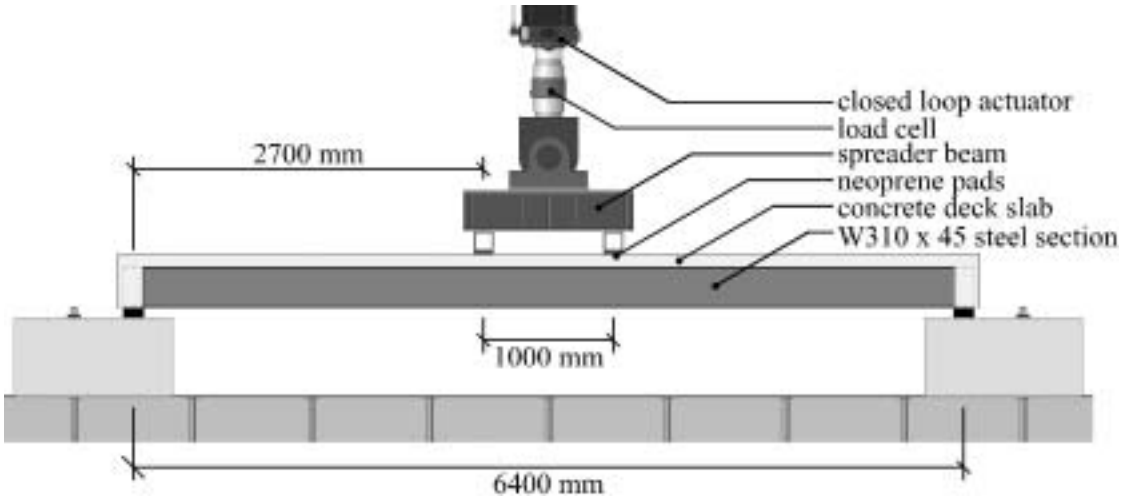

Fig. 2 Loading configuration of large-scale steel-concrete composite beams

2.1.3 Results and Observations

The behavior in the service range was examined by loading each of the beams to a tension strain of 0.12 percent at the bottom of the steel tension flange before and after strengthening. Table 3 shows the results in the elastic range for the three large-scale beams. As was expected, use of higher modulus fiber in conjunction with the highest reinforcement ratio resulted in the highest stiffness increase. For beam HM-3.8-PS strengthened with the prestressed CFRP strip, even though only half the amount of CFRP material was used, a similar stiffness increase was recorded in the elastic range. This takes into account the 2.0 mm of camber that was induced during prestressing before any load was applied to the beam.

Table 3 Stiffness improvements up to an induced strain of 0.12 percent for unstrengthened and strengthened steel-concrete composite beams

		Unstrengthened		Strengthened	
Specimen	Stiffness increase	Load (kN)	Net midspan deflection (mm)	Load (kN)	Net midspan deflection (mm)
IM-4.5-AB	10 %	150	15.8	173	16.3
HM-7.6-AB	36 %	152	15.0	226	16.4
HM-3.8-PS	31 %*	151	15.2	184	14.1*

* accounting for beneficial effect of the camber

The load-deflection behavior of each of the beams to ultimate is shown in Fig. 3. The behavior of each of the three beams was essentially bilinear until rupture of the CFRP strips, with only a slight decrease in stiffness occurring once the steel reached yield. Similar to the findings of Sen *et al.* (2001) and Tavakkolizadeh and Saadatmanesh (2003A), most of the strength increase occurred in the region between yielding of the steel and rupture of the CFRP. No debonding of the CFRP strips was evident, indicating that the bonding and surface preparation technique used was satisfactory.

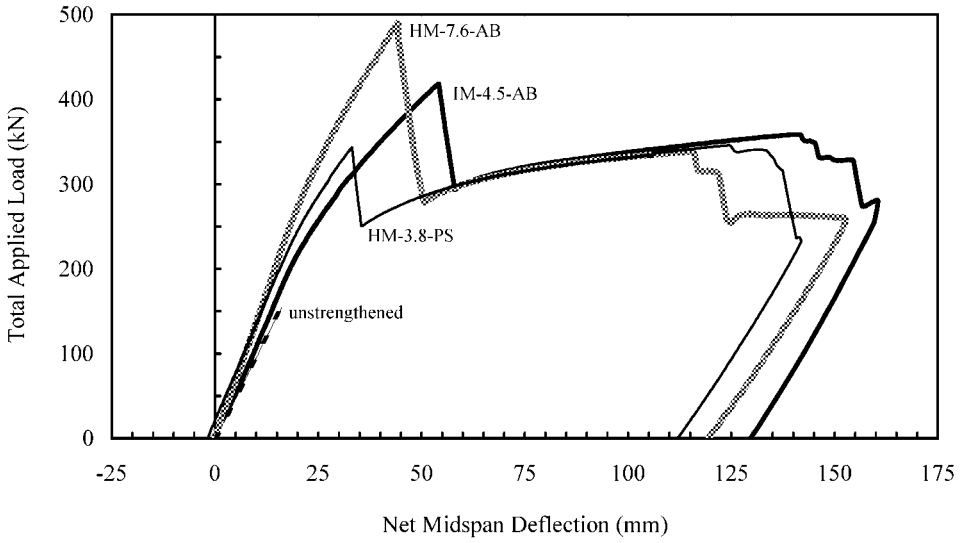

Fig. 3 Load-deflection behavior of the three large-scale beams

Once the strips ruptured, they were no longer effective in strengthening the beams and the beams reverted to their unstrengthened state as evident by the overlap in the load-deflection behavior for all the beams after rupture. Continued loading resulted in concrete crushing. This allows the comparison to be made between the ultimate strength of the strengthened beam at rupture of the CFRP and the strength of the (now unstrengthened) beam at concrete crushing, shown in Fig. 4. For the beams strengthened using the CFRP plates that were not prestressed, increases in ultimate strength were possible, as indicated in Table 4. The prestressed beam was designed to provide the maximum stiffness increase, without increasing the ultimate strength of the section, which may be advantageous in cases where it is desired to maintain the full ductility of the member. This was accomplished by designing the strengthening such that the CFRP strips would rupture near flexural yield of the cross-section.

Table 4 Properties at ultimate for steel-concrete composite beams

		At rupture of the CFRP strips		At concrete crushing	
Specimen	Ultimate strength increase	Load (kN)	Net midspan deflection (mm)	Load (kN)	Net Midspan deflection (mm)
IM-4.5-AB	16 %	418	54.2	359	141.5
HM-7.6-AB	45 %	491	44.3	338	114.6
HM-3.8-PS	none	343	33.1*	346	124.4*

* accounting for beneficial effect of the camber

Fig. 4 Steel-concrete composite beam HM-7.6-AB after failure

2.2 Phase 2: Shear-lag, Overloading and Fatigue Beams

2.2.1 Test Specimens

Seven beams were fabricated to investigate the effect of shear-lag, overloading and fatigue on steel-concrete composite girders strengthened with high modulus CFRP strips. Two different levels of strengthening were considered to examine the effect of reinforcement ratio on the transfer of shear stresses through the adhesive joint, and thus the validity of the assumption that plane sections remain plane. Two beams were used to determine the extent to which strengthening can reduce the damage sustained by a structure in an overload event. Three beams with different reinforcement ratios, tested under the same stress range in the steel tension flange, will be used to examine the fatigue behavior in comparison to a control beam. For this paper only the shear-lag and overloading beams will be reported. The fatigue tests are in progress and will be reported in the presentation. The overloading beams CONT-ST, OVL-1 and OVL-2 were loaded and unloaded at different displacement levels to simulate sever overloading conditions. The test matrix is presented in Table 5.

Table 5 Shear-lag and overloading test matrix

Designation	CFRP type	Reinforcement ratio	Loading
ST-CONT	None	0.0%	Load/Unload
SHL-2	THM-450	8.8%	Monotonic to Failure
OVL-1	THM-450	4.5%	Load/Unload
OVL-2	THM-450	8.8%	Load/Unload

The test specimens, shown schematically in Fig. 5, were fabricated from grade A992 steel W200 x 19 sections. The overall beam length was 3350 mm. Pairs of transverse stiffeners were welded at the supports and at the load points to prevent local web failure. A 65 mm x 525 mm concrete slab was cast on the top of each specimen. The measured concrete strength at 28 days was 43 MPa. Shear interaction between the steel beams and concrete slab was provided by two parallel rows of 12 mm x 50 mm shear studs welded 50 mm apart along the entire length of the beams. The studs were spaced longitudinally at 100 mm on center. The slab was reinforced with 100 mm on center, 6 mm diameter plain welded wire fabric to prevent shrinkage cracking and longitudinal splitting of the deck.

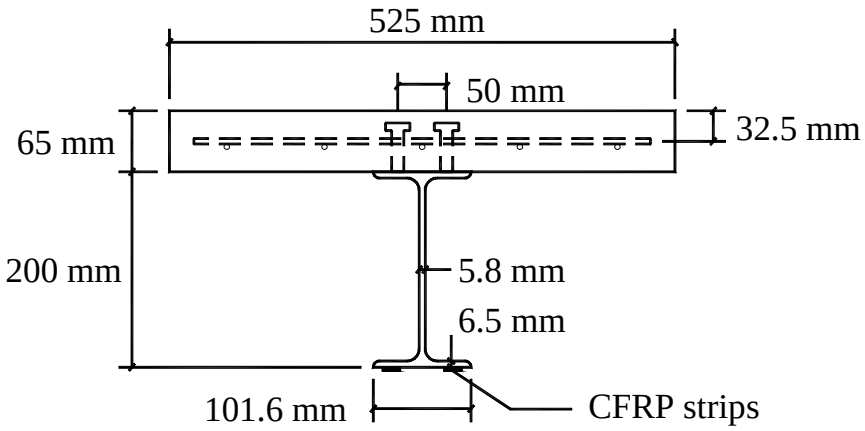

Fig. 5 Schematic of shear-lag and overloading specimens

Beams SHL-2, OVL-1 and OVL-2 were strengthened following the same installation process described previously for the large-scale specimens. A small gap was left between the CFRP strips and between the edge of the CFRP strips and the edge of the steel tension flange to facilitate measurement of strains on the steel tension flange.

2.2.2 Test Procedure

The specimens were tested in four-point bending with a span of 3050 mm and 610 mm between the load points as shown in Fig. 6. A pin and roller support was provided on either end of the beam. Load was applied from a spreader beam to two HSS tubes across the entire deck through neoprene pads in a similar manner to that used for loading of the large-scale beams. The beams were instrumented with electrical resistance strain gauges and strain gauge type displacement transducers gauges to establish the strain profile at mid-span. Beams ST-CONT, OVL-1 and OVL-2 were loaded to predetermined deflection limits and unloaded to determine the extent of damage to the members due to overloading.

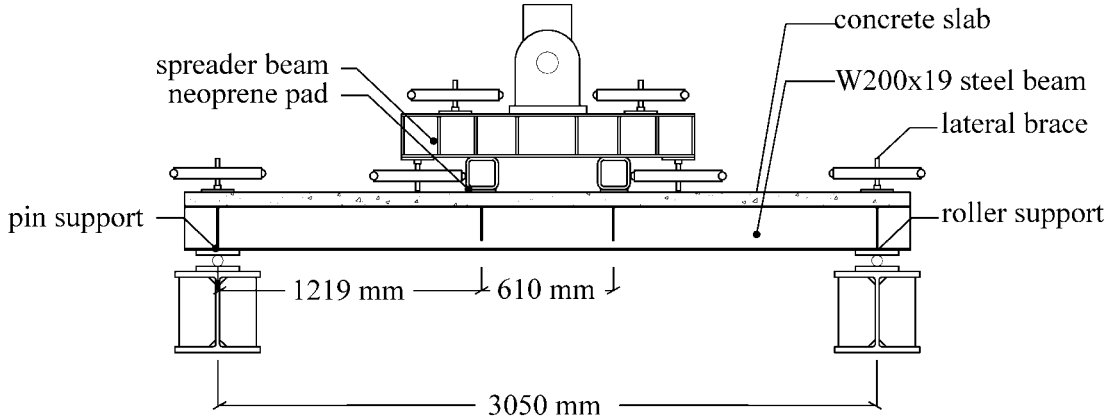

Fig. 6 Loading configuration for small-scale steel-concrete composite beams

2.2.3 Results and Observations

The load deflection relationships of the shear-lag and overloading beams are presented separately in Fig. 7. Rupture of the CFRP occurred at a load of 259 kN for beam OVL-1, and a load of 357 kN for beams OVL-2 and SHL-2. Ultimate failure of the

specimens was due to crushing of the concrete at loads of 216 kN for beams OVL-1 and OVL-2 and 220 kN for beams ST-CONT and SHL-2. Unloading and reloading of specimen ST-CONT was linear with a 7 percent loss in stiffness as compared to the initial member stiffness. Unloading and reloading of specimens OVL-1 and OVL-2 was linear with a 5 percent and 10 percent loss in stiffness respectively prior to rupture of the CFRP. After rupture of the CFRP unloading and reloading remained linear with a post-rupture stiffness equal to that of the unstrengthened member. The higher reinforcing ratio provided a 60 percent ultimate strength increase and a 46 percent stiffness increase while the lower reinforcing ratio provided a 20 percent increase in the ultimate strength and a 26 percent increase in stiffness.

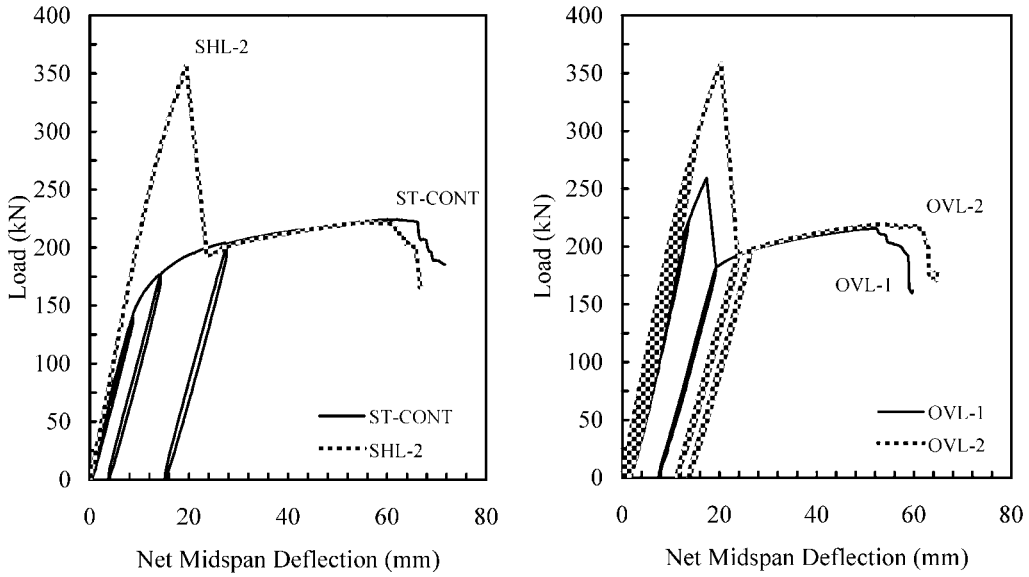

Fig. 7 Load deflection relationships for shear-lag and overloading specimens

Residual deflections were measured after unloading for all three of the overloading beams. Of particular interest is the permanent residual deflection caused by an overloading event, as this can be a measure of the extent of damage sustained by the member. Fig. 8 presents the residual deflection induced after loading to a certain applied load level and unloading to the dead load level. The dead load was selected as the load inducing a stress of $0.3\,f_y$ in the tension flange of the unstrengthened specimen. The service loads for the three specimens, based on an acceptable tension flange strain of $0.6\,f_y$, are also presented. From Fig. 8 it is clear that residual deflections after loading to service load levels for each beam are on the same order of magnitude for the strengthened and unstrengthened beams and are less than L/4000. When the beams were loaded beyond the yield strain of the steel the strengthened specimens exhibited much lower residual deflections in comparison to the control beam.

The effect of shear-lag was determined by considering the strain profiles through the cross-section of the various beams at midspan. Beams ST-CONT and OVL-1 exhibited linear strain profiles at mid-span as expected indicating that shear-lag effects were minimal. Beams SHL-2 and OVL-2, however, exhibited a slight discontinuity at the interface with the CFRP laminates. Fig. 9 presents the mid-span strain profile for

specimens SHL-2 and OVL-2 as measured immediately prior to rupture of the CFRP and the strain profile as determined by a moment-curvature analysis assuming a linear strain profile. The measured strain discontinuity is likely due to residual stresses and local variations of the steel strain due to lateral distortion in the flanges and web of the steel beam, which was confirmed by other instrumentation used in the tests. The different sign convention of the discontinuity of the strain suggests also that the measured discontinuity is not due to the presence of shear-lag.

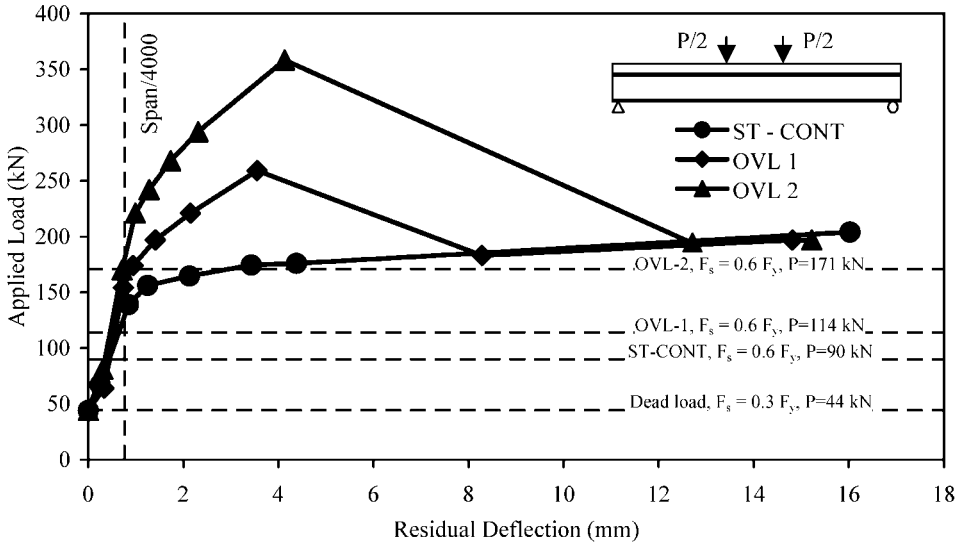

Fig. 8 Residual deflections for overloading specimens

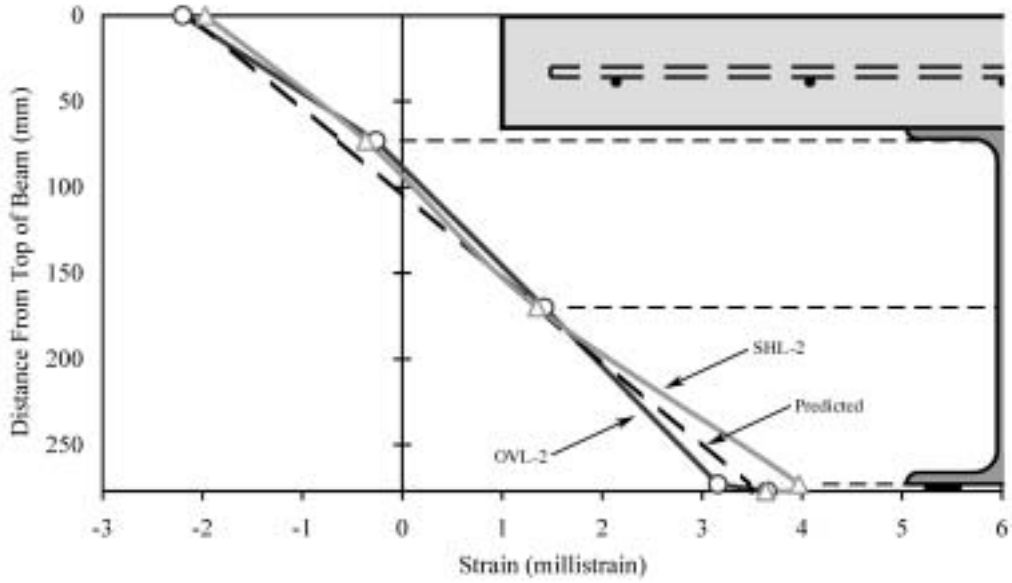

Fig. 9 Strain profiles for specimens SHL-2 and OVL-2

2.2.4 Fatigue Behavior

Three beams similar to those used in the shear-lag and overloading study will used to examine the fatigue behavior of beams strengthened with CFRP. Two beams will be strengthened while the third will remain unstrengthened to serve as a control beam. To simulate actual bridge conditions, a dead load will be applied to induce 0.3 f_y in the

tension flanges of the beams prior to strengthening. The dead load will be maintained throughout the fatigue testing. Preliminary analytical results suggest that live load increases of 30% and 65% can be realized at the two different strengthening levels based on fatigue limitations. Results of these tests will be reported at the conference.

3. CONCLUSIONS

High modulus CFRP material can be used to increase the stiffness and flexural strength of steel-concrete composite flexural members typically used for bridges and structures. The material can be externally bonded to the tension zone or prestressed before being bonded to the tension zone. Use of prestressed CFRP can significantly increase the stiffness under service loading conditions while maintaining the ductility of the original member. The experimental results indicate that the use of high modulus CFRP materials can greatly reduce the overloading damage due to overloading conditions, in comparison to unstrengthened beams loaded to similar stress conditions. Test results indicate that the use of the selected adhesive for the system can achieve excellent bond, with insignificant shear lag at the interface between the steel surface and the high modulus CFRP material.

4. ACKNOWLEDGEMENTS

The authors would like to acknowledge Mitsubishi Chemical America, Inc. in sponsoring this project, and for the financial support provided by the National Science Foundation for the Industry/University Collaborative Research Center, Repair of Buildings and Bridges with Composites (RB^2C), at North Carolina State University.

5. REFERENCES

Brown, A.R.G., (1974): "Corrosion of CFRP to metal couples in saline environments," Proceedings of the 2nd International Conference on Carbon Fibres, London, England, February 18-20, Paper No. 35, pp. 230- 241.

Choqueuse, D., P. Davies, F. Mazeas, R. Baizeau (1997): "Aging of composites in water: Comparison of five materials in terms of absorption kinetics and evolution of mechanical properties," High Temperature and Environmental Effects on Polymeric Composites: 2nd Volume, ASTM Special Technical Publication, 1302, Thomas S. Gates and Abdul-Hamid Zureick, eds., American Society for Testing and Materials, pp. 73-96.

Edberg, William, Dennis Mertz, and John Gillespie, Jr., (1996): "Rehabilitation of steel beams using composite materials," Materials for the New Millennium, Proceedings of the ASCE Fourth Materials Engineering Conference, Washington, D.C., November 10-14, pp. 502-508.

Francis, R. Bimetallic Corrosion, (2000): Guides to Good Practice in Corrosion Control. National Physical Laboratory, Teddington, Middlesex, 15 p.

Gellert, E. P. and D. M. Turley, (1999): "Seawater immersion ageing of glass-fibre reinforced polymer laminates for marine applications," Composites Part A: Applied Science and Manufacturing, v. 30, no. 11, pp. 1259-1265.

Gillespie, J.W., D.R. Mertz, K. Kasai, W.M. Edberg, J.R. Demitz, and I. Hodgson, (1996): "Rehabilitation of steel bridge girders: Large Scale Testing," Proceedings of the American Society for Composites 11th Technical Conference, Atlanta, Georgia, November 4-7, pp. 1249-1257.

Hildebrand, M, (1994): "Non-linear analysis and optimization of adhesively bonded single lap joints between fibre-reinforced plastics and metals," International Journal of Adhesion and Adhesives, v. 14, n. 4, October, pp. 261-267.

Liu, X, P.F. Silva, and A. Nanni, (2001): "Rehabilitation of steel bridge members with FRP composite materials," Proceedings of the International Conference on Composites in Construction, J. Figueiras, L. Juvandes and R. Furia, Eds., Porto, Portugal, October 10-12, pp. 613-617.

Mays, G.C. and A.R. Hutchinson, (1992): Adhesives in Civil Engineering. Cambridge University Press, New York, New York.

McBagonluri, F., K. Garcia, M. Hayes, N. Verghese and J. J. Lesko, (2000): "Characterization of Fatigue and Combined Environment on Durability Performance of Glass/Vinyl Ester Composite for Infrastructure Applications," International Journal of Fatigue, v. 22, no. 1, January, pp. 53-64.

Miller, Trent C., Michael J. Chajes, Dennis R. Mertz and Jason N. Hastings, (2001): "Strengthening of a steel bridge girder using CFRP plates," Journal of Bridge Engineering, ASCE, v. 6, n. 6, November/December, pp. 514-522.

Miriyala, S.K., W.C. Tucker, T.J. Rockett, and R. Brown, (1992): "Degradation of carbon reinforced polymer composites under galvanic coupling conditions," Proceedings of the 33rd AIAA/ASME/ASCE/AHS/ASC Structures, Structural Dynamics, and Materials Conference, Dallas, Texas, April 13-15, pp. 3036-3045.

Sen, Rajan, Larry Liby, and Gray Mullins, (2001): "Strengthening steel bridge sections using CFRP laminates," Composites Part B: Engineering, v. 32, n. 4, pp. 309-322.

Tavakkolizadeh, M. and H. Saadatmanesh, (2001A): "Repair of cracked steel girder using CFRP sheet," Creative Systems in Structural and Construction Engineering, Proc. of the 1st International Structural Engineering and Construction Conference, Amarjit Singh, ed., Honolulu, Hawaii, January 24-27, pp. 461-466.

Tavakkolizadeh, Mohammadreza and Hamid Saadatmanesh, (2001B): "Galvanic corrosion of carbon and steel in aggressive environments," Journal of Composites for Construction, v. 5, n. 3, August, pp 200-2

Tavakkolizadeh, M. and H. Saadatmanesh, (2003A): "Strengthening of steel-concrete composite girders using carbon fiber reinforced polymer sheets," Journal of Structural Engineering, ASCE, v. 129, n. 1, January, pp. 30-40.

Tavakkolizadeh, M. and H. Saadatmanesh, (2003B): "Fatigue strength of steel girders strengthened with carbon fiber reinforced polymer patch," Journal of Structural Engineering, ASCE, v. 129, n. 2, February, pp. 186-196.